**TELKOMNIKA Telecommunication, Computing, Electronics and Control**
Vol. 19, No. 5, October 2021, pp. 1594~1604
ISSN: 1693-6930, accredited First Grade by Kemenristekdikti, Decree No: 21/E/KPT/2018
DOI: 10.12928/TELKOMNIKA.v19i5.20063 

# Classification of water stress in cultured Sunagoke moss using deep learning

**Yusuf Hendrawan, Retno Damayanti, Dimas Firmanda Al Riza, Mochamad Bagus Hermanto**
Department of Agricultural Engineering, Laboratory of Mechatronics and Agro-industrial Machineries, Universitas Brawijaya, Malang, Indonesia

**Article Info**

***Article history:***

Received Feb 17, 2021
Revised Jul 14, 2021
Accepted Aug 3, 2021

***Keywords:***

Convolutional neural network
Cultured Sunagoke moss
Machine vision
Non-destructive sensing
Water stress

**ABSTRACT**

Water stress greatly determines plant yield as it affects plant metabolism, photosynthesis rate, chlorophyll content index, number of leaves, physiological, biochemical compound, and vegetative growth. The research aimed to detect and classify water stress of cultured Sunagoke moss into several categories i.e. dry, semi-dry, wet, and soak by using a low-cost commercial visible light camera combined with a deep learning model. Cultured Sunagoke moss is a commercial product which has the potential use as rooftop-greening and wall-greening material. This research compared the performance of four convolutional neural network models, such as SqueezeNet, GoogLeNet, ResNet50, and AlexNet. The best convolutional neural network model according to the training and validation result was ResNet50 with RMSProp optimizer, 30 epoch, and 128 mini-batch size; this also gained an accuracy rate at 87.50%. However, the best result of the convolutional neural network model on data testing using confusion matrices on different data sample was ResNet50 with Adam optimizer, 30 epoch, 128 mini-batch size, and average testing accuracy of 94.15%. It can be concluded that based on the overall results, convolutional neural network model seems promising as a smart irrigation system that real-time, non-destructive, rapid, and precise method when controlling water stress of plants.



***Corresponding Author:***

Yusuf Hendrawan
Department of Agricultural Engineering
Universitas Brawijaya
Veteran St., Malang, Indonesia
Email: yusuf_h@ub.ac.id

## 1. INTRODUCTION

Environmental conditions such as temperature, humidity, carbon dioxide, light intensity, water, and nutrient solution greatly affect plants growth [1]. Optimum environmental conditions can increase plant growth and productivity. However, if one of those environmental factors is not optimum, then it leads to plant stress. Water stress comes into a major concern among various types of stress in plants due to its implication [2]. It can affect plants metabolism and further influence plant growth and development which also can reduce plants productivity [3]. When water stress in plants occurs, the chemical signals are transmitted from root to leaf through the xylem which can stimulate closure of stomata and lower photosynthesis performance. Maseko *et al.* [4] has investigated water stress on several plants (*Amaranthus cruentus* L., *Corchorus olitorius* L, and *Vigna unguiculata* (L.) Walp and *Beta vulgaris* L.) affected plant height, chlorophyll content index, yield, and the number of leaves. Moreover, Hendrawan and Murase [5]

proved that water stress in moss plants corresponded to its photosynthesis rate. Water stress defines as a condition where plants experience either lack or excess of water than its requirement. Zhang *et al.* [6] observed that water stress affected root biomass and secondary metabolites on the *Stellaria dichotoma* L.*var. lanceolata* Bge. Ibrahim and Abdellatif [7] in their research concluded that water stress in wheat plants (*Triticum aestivum* L. cv. *Giza* 168) reacted on the biochemical components such as phenolic compounds, flavonoids, amino acids, sugars, total soluble sugars, protein, and more. Furthermore, it has been shown that water stress affected the antimicrobial activity of some medicinal plants [8]. And more, water stress contributed to the vegetative growth, yield, and quality of potato plants [9]. Sun *et al.* [10] in his research found evidence that water stress affected the relative growth rate of some types of marsh herbaceous plants. Jiang *et al.* [11] also proved that it influenced both linearly and non-linearly on plants' height and elongation rate of winter wheat. Ju *et al.* [12] revealed the effect of water stress on the physiological, micro-morphological, and metabolomics on the grape vines. According to the water stress impacts on plants mentioned, it is urgent to develop methods that can detect water stress in plants accurately for assuring optimal plant growth. The water stress detection method in plants is determined by two majors: instrumentation (sensor) and modeling method. Rapid, real-time, and non-destructive sensing are principal in detecting water stress in plants.

Water stress detection methods in plants have been widely developed such as spectral reflectance of plant leaves using spectrometer [13]. In research conducted by Ihuoma and Madramootoo [14], the spectral reflectance using fiber-optic spectrometer ranging from 200 nm to1150 nm can detect water stress in potato plants. Liu *et al.* [15] used a thermal camera to detect water stress in *Eucalyptus microcarpa* and *Acacia pycnantha* plants according to thermal indices of the leaf canopy. Khorsandi *et al.* [16] has also been successfully detected water stress in sesame plants using infrared thermography. Moreover, previous studies have widely used visible near-infrared (VIS/NIR) spectroscopy to detect water stress in plants [17], as research conducted by Xia [18], she used VIS/NIR to detect it in tomato plants. Furthermore, Fonseca *et al.* [19] was successful to detect water stress in blueberry plants non-destructively using VIS/NIR with the highest $R^2$ 0.69. Terahertz spectroscopy also became alternatives for non-destructive sensing to detect water stress in plants as carried out by Li [20]. She has successfully measured leaf water content in soybean plants using terahertz time-domain spectroscopy. Another non-destructive method that has been developed to detect water stress in plants is by using laser-induced fluorescence technology. This method was successfully applied in *Arabidopsis* plants [21]. Hyperspectral machine vision was investigated and proven effective to detect water stress in tomato plants [22]. A simpler and cheaper machine vision method using a low-cost commercial visible-light camera was also researched and proven effective to detect water stress in plants in a rapid and non-destructive way [23]-[25].

Artificial intelligence utilization as a model in predicting water stress on plants has been widely carried out by researchers. Wakamori *et al.* [26] used a multimodal neural network with a clustering-based drop (C-drop) to predict water stress in plants accurately with the highest $R^2$ 0.429. This model can be used for decision making for an irrigation system and proven precise and stable to detect water stress in plants. Kaneda *et al.* [27] used multi-modal sliding window-based support vector regression to predict water stress in plants with prediction effectiveness showed by the highest R-value accounting for 0.509. The least-squares vectors machine was investigated and proven effective for classifying some water stress categories in wheat plants [28]. Hendrawan and Murase [29] inspected artificial neural network (ANN) effectiveness to predict water stress in moss plants root mean square error (RMSE) with its validation accuracy of 0.0107. Although only a few researches on deep learning propose this will bring many possibilities for future research in detecting stress in plants [30]. As Anami *et al.* [31], who proposed the method to classify water stress in paddy crop resulting in training data accuracy of 92.89%. Other researchers using deep learning to detect stress on nitrogen deficiency in sorghum plants with an accuracy of 92% [32] and convolutional neural network (CNN) use to detect light stress in lettuce with an accuracy of 87.95% [33]. This kind of deep learning, CNN, showed an outstanding performance in image recognition scope and therefore this may bring potential methods to detect water stress in plants compared to other machine learning methods. A low-cost commercial visible light camera combined with deep learning will create a robust alternative method as it is rapid, real-time, non-destructive, accurate, and affordable. Such a combination has not been widely developed in research.

The research aims to detect and classify water stress in the cultured Sunagoke moss *Rhacomitrium japonicum* into several categories (dry, semi-dry, wet, and soak) by using a low-cost commercial visible light camera tool and deep learning model. The result of the method developed can later be utilized to optimize irrigation control in the production of cultured Sunagoke moss in plant factory (closed bio-production system) so it can grow more optimal. Sunagoke moss which under water stress conditions i.e. lack of water (dry and semi-dry) or excess of water (soak) cannot photosynthesize optimally and certainly affect the yield.

Cultured Sunagoke moss is a very potential commercial product to use as rooftop-greening and wall-greening material.

## 2. RESEARCH METHOD

Sunagoke moss sample (500×500 mm, M-300, VARORE Co., Japan) consisting of several water stress conditions, dry (0-1 g $g^{-1}$), semi-dry (1-2 g $g^{-1}$), wet (2-3 g $g^{-1}$), and soak (>3 g $g^{-1}$) were set where g $g^{-1}$ is water weight (g) per initial dry weight (g). Figure 1 shows the moss sample. The water content of moss samples was set by initial dry weight. All moss samples were put on the growth chamber (Biotron NK 350, Japan) at optimal environmental condition, air temperature=15 °C, RH=80%, $CO_2$=400 ppm, light intensity=86.5 mol $m^{-2}s^{-1}$, and light duration=12 h. Each moss sample was given water to 4 g $g^{-1}$ and allowed to dry to reach its initial dry weight. Generally, moss grows optimally at water content 2-3 g $g^{-1}$ (wet condition). The sample moss image was acquired using a visible light commercial digital camera (Nikon Coolpix SQ, Japan). The initial image resolution size was 1024×768 pixels, then, reduced to 300×300 pixels. 200 images of each water stress category were captured producing a total of 800 images from four categories. 70% of 800 (560 images) were set for training data and the rest 30% (240 images) for validation data. Data testing was also required as a final model assessment taken separately at different times with a total of 240 moss image data under different water stress conditions.

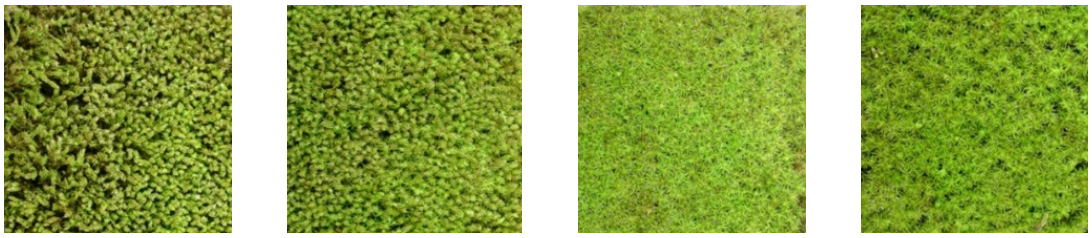

(a) (b) (c) (d)

Figure 1. 300×300 pixels image of moss in different water stress: (a) dry; (b) semi-dry; (c) wet; (d) soak

CNN, one of deep learning methods, has become popular to solve computer vision-based agricultural problem [34]. Compare with other machine learning methods, as fundamental difference, feature extraction process is omitted in CNN. Instead, it can directly manage raw image to classify output by tuning the parameters in convolutional and pooling layers. In the classification process, deep learning architecture was used to classify sample moss image in four water stress stages i.e. dry, semi-dry, wet, and soak. Structure of typical CNN can be seen in Figure 2. CNN structures covered image acquisition, convolutional layer, pooling layer, and fully connected layer. The research used the deep learning application with four types of pretrained CNN models (SqueezeNet [35], GoogLeNet [36], Resnet50 [37], and AlexNet [38]) provided in MATLAB R2020b platform.

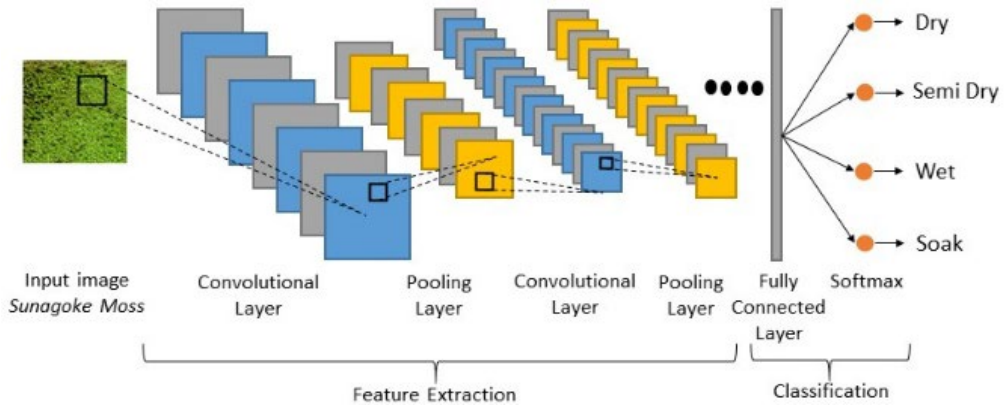


Figure 2. Proposed computer vision for classifying water stress in cultured moss using deep learning

Figure 3 (a) shows SqueezeNet architecture details with processing stages including: 1) resizing the image data into 227×227 pixels with depth 3 (RGB channels); 2) convolutions with stride [2 2] and padding [0 0 0 0]; 3) max pooling with stride [2 2] and padding [0 0 0 0]; 4) max pooling with stride [2 2] and padding [0 1 0 1]; 5) 2-steps fire module with stride [1 1] and padding [0 0 0 0]; 6) max pooling with stride [2 2] and padding [0 1 0 1]; 7) 4-steps fire module with stride [1 1] and padding [0 0 0 0]; 8) convolutions with 4 output, stride [1 1], and padding [0 0 0 0]; 9) average pooling; and 10) output.

Figure 3 (b) shows GoogLeNet architecture details with processing stages including: 1) resizing the image data into 224×224 pixels with depth 3; 2) convolutions with stride [2 2] and padding [3 3 3 3]; 3) max pooling with stride [2 2] and padding [0 1 0 1]; 4) convolutions with stride [1 1] and padding [0 0 0 0]; 5) convolutions with stride [1 1] and padding [1 1 1 1]; 6) max pooling with stride [2 2] and padding [0 1 0 1]; 7) 2-steps inception module; 8) max pooling with stride [2 2] and padding [0 1 0 1]; 9) 5-steps inception module; 10) max pooling with stride [2 2] and padding [0 1 0 1]; 11) 2-steps inception module; 12) average pooling; 13) fully connected layer with 4 output; 14) output.

Figure 3 (c) shows ResNet50 architecture details consisting of 34 layers with one additional max pooling layer at the beginning and one average pooling layer at the end. The architecture details including: 1) resizing the image data into 224×224 pixels with depth 3; 2) convolutions with stride [2 2] and padding [3 3 3 3]; 3) batch normalization convolutions; 4) max pooling with stride [2 2] and padding [1 1 1 1]; 5) residual block ×16; 6) average pooling; 7) fully connected layer with 4 output; 8) output.

Figure 3 (d) shows AlexNet architecture details consisting of 8 layers with 5 convolutional layers and 3 fully connected layers which each convolutional layer was combined with max pooling layer and one normalization layer in order to reduce the image resolution size and to normalize image resultant value. The architecture details include: 1) resizing the image data into 227×227 pixels with depth 3; 2) convolutions with stride [4 4] and padding [0 0 0 0]; 3) max pooling with stride [2 2] and padding [0 0 0 0]; 4) convolutions with stride [1 1] and padding [0 0 0 0]; 5) max pooling with stride [2 2], and padding [0 0 0 0]; 6) 3-steps convolutions with stride [1 1] and padding [1 1 1 1]; 7) max pooling with stride [2 2] and padding [0 0 0 0]; 8) 3-steps fully connected layer with 4 output; 9) output. ReLu activation function was used in every hidden layer and softmax function was applied in the final layer to ensure the output values to constantly range between 0 and 1.

ReLu activation function is given as:

$$f(x) = \max(0, x) \quad (1)$$

Softmax activation function is given as:

$$f(x_i) = \sum \frac{e^{x_i}}{e^{x_k}} \quad (2)$$

In the training process, the maximum epoch was set at the values of 20 and 30; mini-batch size was set at the values of 20 and 128, iteration per epoch at the values of 4 and 28, maximum iteration at the values of 120 and 560, the momentum of 0.9, and loss function used binary cross-entropy. Research conducted by Thenmozhi and Reddy [39] stated that the best learning rate of the CNN model was 0.0001; thus, the research set the initial learning rate at 0.0001. Moreover, the study used the following optimization techniques (optimizer): stochastic gradient descent with momentum (SGDm), adaptive moment estimation (Adam), and root mean square propagation (RMSProp) [40]. SGDm accelerated the convergence by replacing actual gradients with estimation, calculated from a randomly selected subset of data. Adam is an algorithm to optimize learning rate by combining the advantage of RMSProp and SGDm. In this research, augmentation data were also used to increase the data number by applying rotation (min=0; max=90) and rescaling (min=1; max=2). CNN program was run on a computer with the following specifications, Intel Core i3-4150 CPU @3.50 GHz (4 CPUs) 10 GB of RAM. Performances of 24 types of CNN models built were later evaluated based on the data accuracy and validation to take 5 best CNN models. The performance of those 5 best CNN models was tested according to the classification using confusion matrices which used data testing. The accuracy of each CNN model was the main parameter that determines performance by the following equation:

$$Accuracy = \frac{number\ of\ correct\ prediction}{total\ number\ of\ samples\ used\ for\ prediction} \quad (3)$$

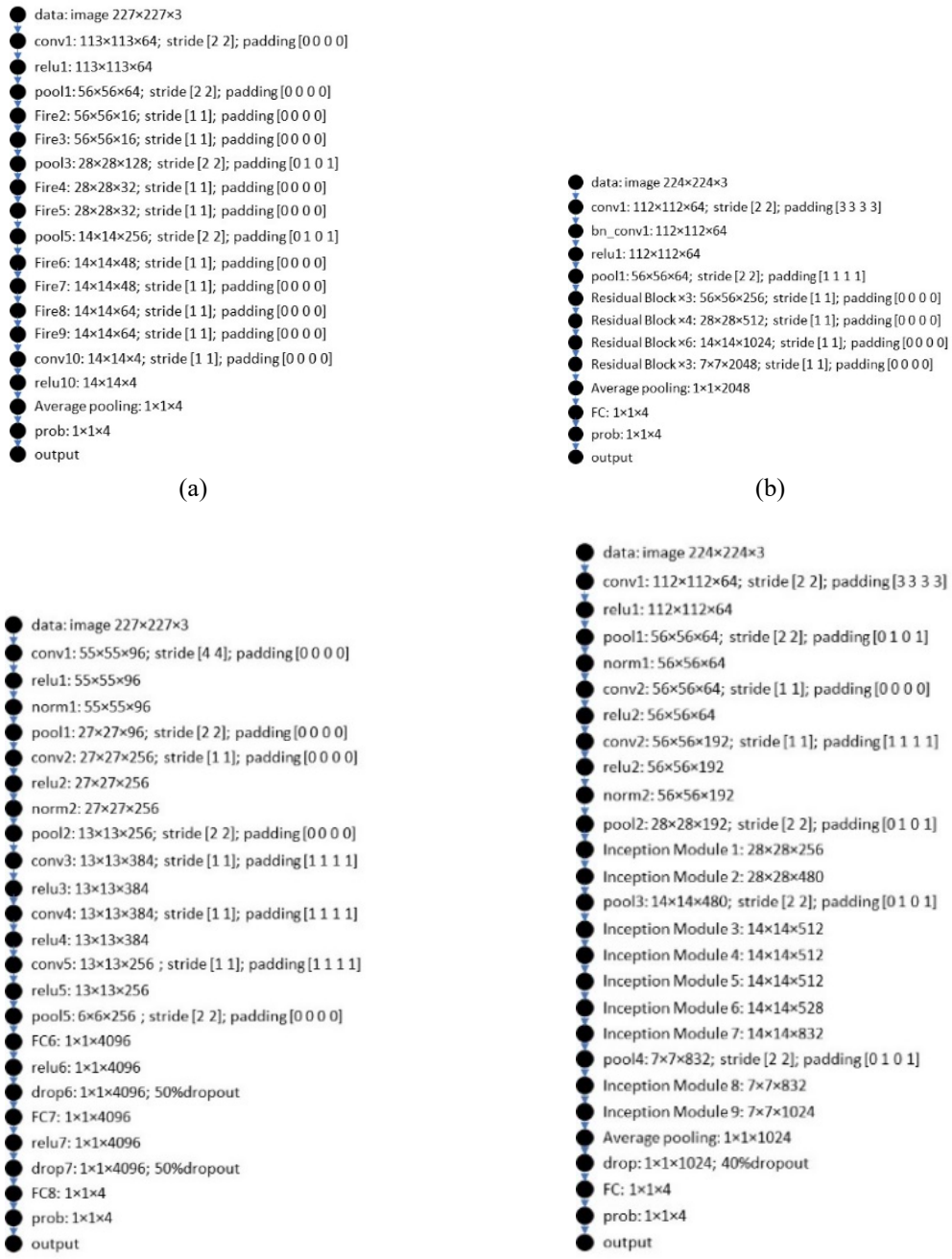


Figure 3. Schematic representation of CNN model: (a) SqueezeNet; (b) ResNet50; (c) AlexNet; (d) GoogLeNet

## 3. RESULTS AND ANALYSIS

Based on those 24 types of CNN models to classify water stress in moss plants, it acquired the accuracy value of data validation ranging from 58.33% to 87.50%. CNN model with a different number of layers affected prediction accuracy of water stress classification in cultured Sunagoke moss. Furthermore, the choice of optimization technique also influenced prediction accuracy. Table 1 shows the accuracy result of validation data resulted from the learning process that used deep learning architecture. Sensitivity analysis was carried out by tuning the optimization technique, maximum epoch, and mini-batch size for each CNN model i.e. SqueezeNet, GoogLeNet, ResNet50, and AlexNet. However, not all CNN models evidently produced performance with high accuracy value. The highest accuracy values gained by each model were presented in Table 1.

Table 1. Results and parameters used in deep learning

| Architecture | Optimizer | Epoch | Mini-batch Size | Max Iteration | Accuracy (%) | Training Time (minutes) |
|---|---|---|---|---|---|---|
| SqueezeNet | SGDm | 30 | 128 | 120 | 64.17 | 27 |
| | Adam | 30 | 128 | 120 | 70.83 | 29 |
| | RMSProp | 30 | 128 | 120 | 69.58 | 29 |
| | SGDm | 20 | 20 | 560 | 65 | 36 |
| | Adam | 20 | 20 | 560 | 72.08 | 35 |
| | RMSProp | 20 | 20 | 560 | 58.33 | 35 |
| GoogLeNet | SGDm | 30 | 128 | 120 | 67.08 | 54 |
| | Adam | 30 | 128 | 120 | 62.08 | 53 |
| | RMSProp | 30 | 128 | 120 | 63.75 | 53 |
| | SGDm | 20 | 20 | 560 | 74.17 | 90 |
| | Adam | 20 | 20 | 560 | 84.17 | 78 |
| | RMSProp | 20 | 20 | 560 | 78.75 | 80 |
| ResNet50 | SGDm | 30 | 128 | 120 | 70 | 848 |
| | Adam | 30 | 128 | 120 | 86.67 | 713 |
| | RMSProp | 30 | 128 | 120 | 87.5 | 701 |
| | SGDm | 20 | 20 | 560 | 78.75 | 187 |
| | Adam | 20 | 20 | 560 | 77.5 | 191 |
| | RMSProp | 20 | 20 | 560 | 77.08 | 199 |
| AlexNet | SGDm | 30 | 128 | 120 | 73.75 | 20 |
| | Adam | 30 | 128 | 120 | 65.42 | 17 |
| | RMSProp | 30 | 128 | 120 | 63.75 | 17 |
| | SGDm | 20 | 20 | 560 | 63.33 | 43 |
| | Adam | 20 | 20 | 560 | 59.17 | 40 |
| | RMSProp | 20 | 20 | 560 | 60 | 46 |

Five CNN models with highest accuracy value were reached by Resnet50 (optimizer=RMSProp, epoch=30, mini-batch size=128), ResNet50 (optimizer=Adam, epoch=30, mini-batch size=128), GoogLeNet (optimizer=Adam, epoch=20, mini-batch size=20), GoogLeNet (optimizer=RMSProp, epoch=20, mini-batch size=20), and ResNet50 (optimizer=SGDm, epoch=20, mini-batch size=20) with accuracy value of each validation data as follows, 87.50%, 86.67%, 84.17%, 78.75%, and 78.75%, respectively. The best performance of the 5 CNN models can be seen in Appendix. This (see Appendix) illustrates the comparison between classification accuracy and loss on the number of iterative learning. Based on the performance result, it was obvious that performance continuously improves as the iteration increases. According to the CNN performance graphic, it was also seen that the accuracy improved as the iteration increased, conversely, the loss graphic decreased as the iteration increased and the longer seen the more convergent it is. All CNN models have relatively the same pattern; the performance improvement run very fast in the initial epoch between epoch 1 to epoch 10 and the accuracy value was slowly increased followed by minor improvement both in data training performance and validation data. According to all results in Appendix, it can be seen some parameters i.e. optimization technique, epoch number, mini-batch size, and iteration number affected the accuracy result of validation data. From the research result, it is seen that as epoch value increased, the accuracy performance did so. The bigger value of mini-batch size affected the longer a model to run, and also influenced memory needs.

Figure 4 illustrates confusion matrices result by using data testing on five best CNN models such as GoogLeNet (optimizer=Adam, epoch=20, mini-batch size=20); GoogLeNet (optimizer=RMSProp, epoch=20, mini-batch size=20); ResNet50 (optimizer=Adam, epoch=30, mini-batch size=128); Resnet50 (optimizer=RMSProp, epoch=30, mini-batch size=128); and ResNet50 (optimizer=SGDm, epoch=20, mini-batch size=20). Individual classification rate for every category was described by comparing predicted value (abscissa) and true value (ordinate). The value distribution of the confusion matrices on the five best CNN models showed the trend of dry class and semi-dry class to have higher accuracy than the other two classes with data testing average of 88.00% for dry class and 89.66% for semi-dry class. In dry moss condition, it was clear that plants have roughest surface texture and browning effects on the tip of plants stalk due to dryness. It is in agreement with the research by Miranda [41] that level of dryness resulted in browning in plants. In semi-dry moss conditions, the moss has a rather rough surface texture and slightly browning effects on the tip of plants. The surface texture between dry and semi-dry moss was rather difficult to distinguish due to their almost similar rough texture and have a deeper green color. The moss plants showed in reverse when in wet condition, they appeared to have a relatively soft surface texture with a lighter green color, and almost no browning effect in this condition. Moreover, it was nearly the same in wet condition, the moss in soak class also had a very soft surface texture so as the result of those conditions were also difficult to distinguish. Accordingly, overall classification accuracy in wet and soak were lower than in other classes. Yet, each CNN model had different result characteristics of confusion matrices in detail. In all CNN models using GoogLeNet appeared that the wet and soak conditions had the highest accuracy value than other conditions that is 100%. In the CNN model using ResNet50, semi-dry conditions tended to have

the highest accuracy. If it is based on the accuracy result of data testing using confusion matrices, it can be concluded that the highest accuracy was reached by CNN model using ResNet50 (optimizer=Adam, epoch=30, mini-batch size=128) with the average accuracy value of 94.15%, followed by Resnet50 (optimizer=RMSProp, epoch=30, mini-batch size=128), ResNet50 (optimizer=SGDm, epoch=20, mini-batch size=20), GoogLeNet (optimizer=RMSProp, epoch=20, mini-batch size=20), and GoogLeNet (optimizer=Adam, epoch=20, mini-batch size=20) with the average accuracy value consecutively 88.75%, 83.77%, 80.4%, and 78.33%. By the highest average accuracy of 94.15%, the CNN model produced in this research can be utilized effectively to classify water stress conditions in cultured Sunagoke moss. In the future work, it can further continue for irrigation plants control application both in the greenhouse (semi-closed bio-production system) and in the plant factory (fully closed bio-production system). With the CNN model, a rapid, real-time, and precise control system can be achieved. Thus, high-quality plant products and productivity can be obtained. This can also be used as a basis for developing a CNN model to detect and predict various kinds of stress on other various types of plants.

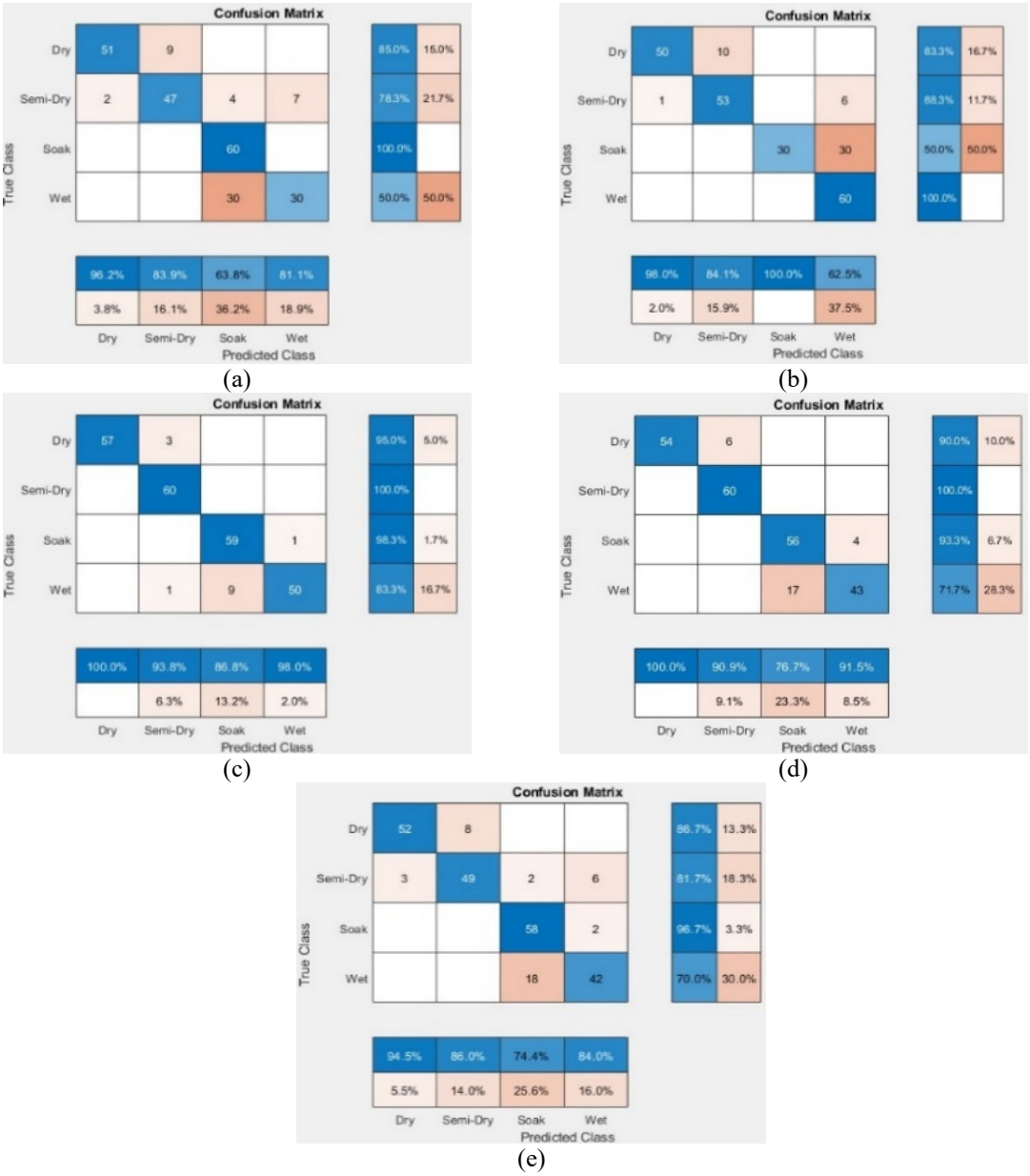


Figure 4. Confusion matrices of testing data: (a) GoogLeNet (optimizer = Adam, epoch = 20, mini-batch size=20); (b) GoogLeNet (optimizer=RMSProp, epoch=20, mini-batch size=20); (c) ResNet50 (optimizer=Adam, epoch=30, mini-batch size=128); (d) Resnet50 (optimizer=RMSProp, epoch=30, mini-batch size=128); (e) ResNet50 (optimizer=SGDm, epoch=20, mini-batch size=20).

## 4. CONCLUSION

This research used four types of CNN model namely SqueezeNet, GoogLeNet, ResNet50, and AlexNet to classify four types of water stress in cultured Sunagoke moss namely dry, semi-dry, wet, and soak. Based on the training and validation result, it obtained accuracy value ranging from 58.33% to 87.50%. The highest accuracy value was obtained when using Resnet50 model with the following settings, optimizer parameter=RMSProp, maximum epoch=30, and mini-batch size=128. However, according to the data testing test result of different moss plant samples, ResNet50 model with the settings, parameter optimizer=Adam, maximum epoch=30, and mini-batch size=128 resulted the highest testing accuracy 94.15%. Therefore, it can be concluded that the CNN model resulted in this research can be effectively used to classify water stress condition in cultured Sunagoke moss. Then, the model can create rapid, real-time, precise, and non-destructive irrigation control system in plants to avoid water stress either lack or excess of water.

## APPENDIX

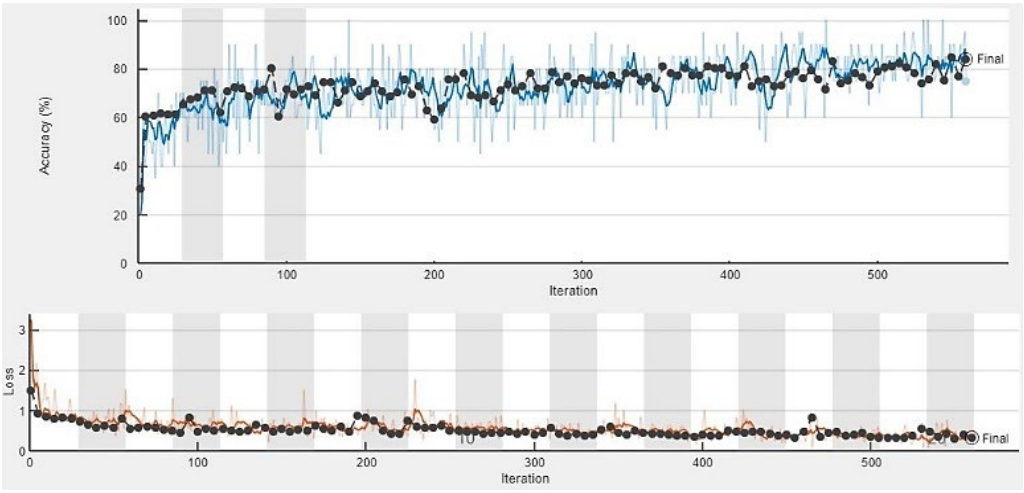


(a)

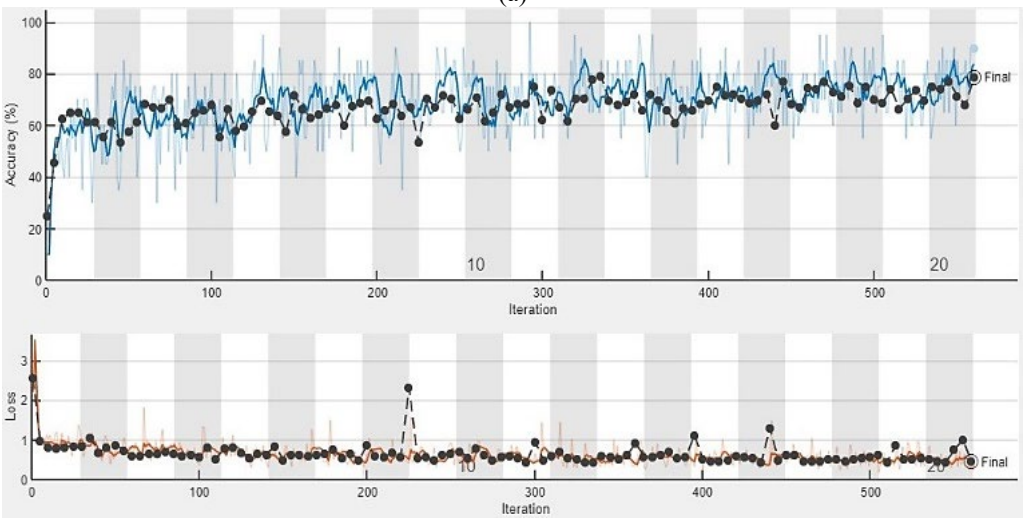


(b)

Accuracy and loss versus the number of iterations; (a) GoogLeNet (optimizer=Adam, epoch=20, mini-batch size=20); (b) GoogLeNet (optimizer=RMSProp, epoch=20, mini-batch size=20);

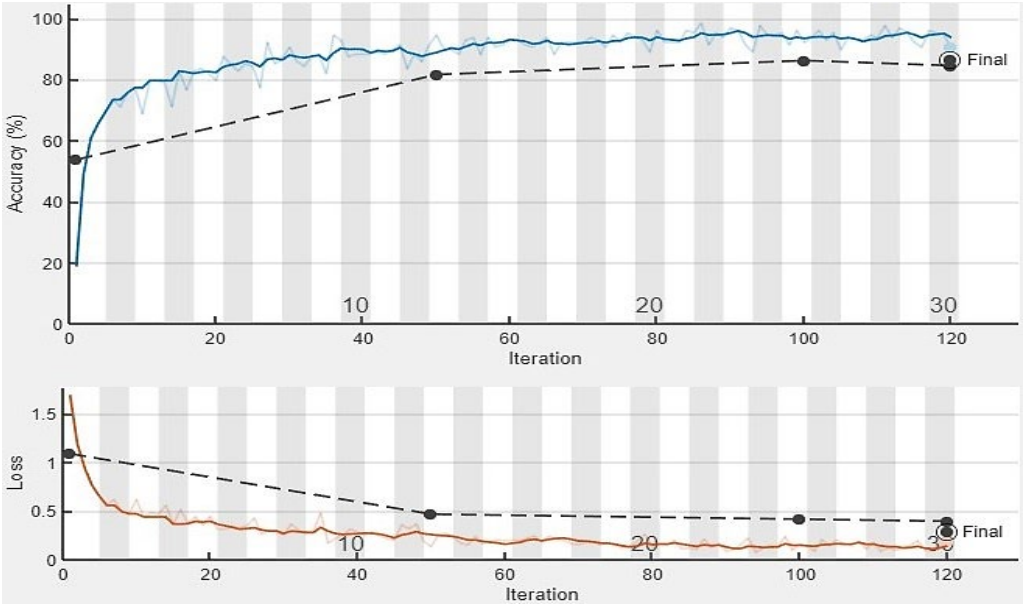


(c)

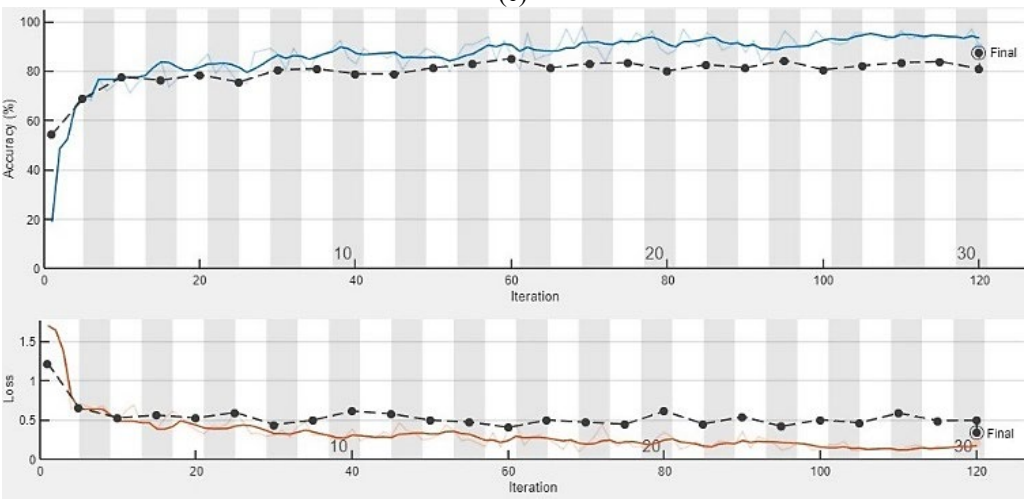


(d)

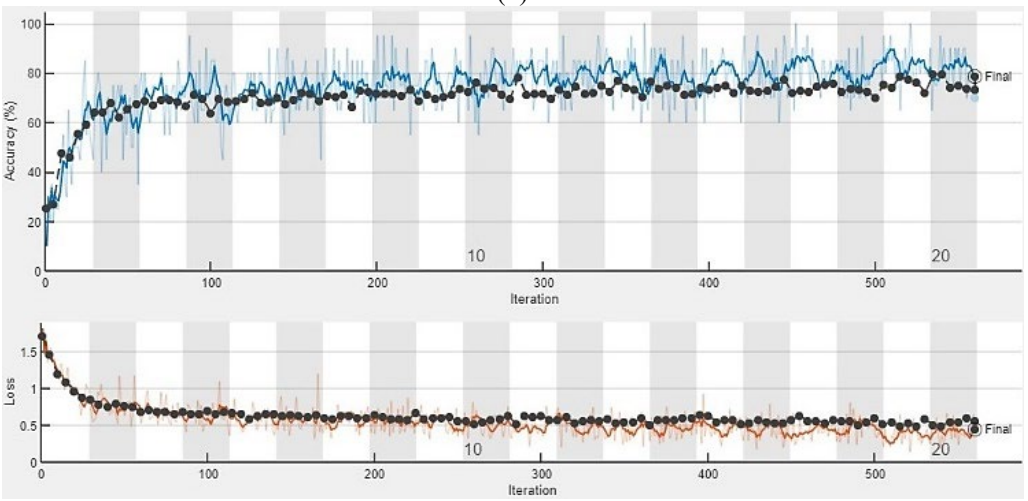


(e)

Accuracy and loss versus the number of iterations; (c) ResNet50 (optimizer=Adam, epoch=30, mini-batch size=128) (d) Resnet50 (optimizer=RMSProp, epoch=30, mini-batch size=128); (e) ResNet50 (optimizer=SGDm, epoch=20, mini-batch size=20)

## REFERENCES


[1] K. L. Huang, C. L. Yang, and C. M. Kuo, "Plant factory crop scheduling considering volume, yield changes and multi-period harvests using Lagrangian relaxation," *Biosystems Engineering,* vol. 200, pp. 328-337, Dec. 2020, doi: 10.1016/j.biosystemseng.2020.10.012.

[2] E. T. Albergaria, A. F. M. Oliveira, and U. P. Albuquerque, "The effect of water deficit stress on the composition of phenolic compounds in medicinal plants," *South African Journal of Botany,* vol. 131, pp. 12-17, Jul. 2020, doi: 10.1016/j.sajb.2020.02.002.

[3] M. Kulak, J. V. J. Novo, M. C. R. Rodriguez, E. D. Yildirim, F. Gul, and S. Karaman, "Seed priming with salicylic acid on plant growth and essential oil composition in basil (Ocimum basilicum L.) plants grown under water stress conditions," *Industrial Crops and Products,* vol. 161, pp. 113235, Mar. 2021, doi: 10.1016/j.indcrop.2020.113235.

[4] I. Maseko *et al.*, "Moisture stress on physiology and yield of some indigenous leafy vegetables under field conditions," *South African Journal of Botany,* vol. 126, pp. 85-91, Nov. 2019, doi: 10.1016/j.sajb.2019.07.018.

[5] Y. Hendrawan and H. Murase, "Precision irrigation for Sunagoke moss production using intelligent image analysis," *Environment Control in Biology,* vol. 47, no. 1, pp. 21-36, Feb. 2009, doi: 10.2525/ecb.47.21.

[6] W. Zhang *et al.*, "Effect of water stress on roots biomass and secondary metabolites in the medicinal plant Stellaria dichotoma L. var. lanceolata Bge," *Scientia Horticulturae,* vol. 224, pp. 280-285, Oct. 2017, doi: 10.1016/j.scienta.2017.06.030.

[7] H. A. Ibrahim and Y. M. R. Abdellatif, "Effect of maltose and trehalose on growth, yield and some biochemical components of wheat plant under water stress," *Annals of Agricultural Sciences,* vol. 61, no. 2, pp. 267-274, Dec. 2016, doi: 10.1016/j.aoas.2016.05.002.

[8] T. R. Netshiluvhi and J. N. Eloff, "Effect of water stress on antimicrobial activity of selected medicinal plant species," *South African Journal of Botany,* vol. 102, pp. 202-207, Jan. 2016, doi: 10.1016/j.sajb.2015.04.005.

[9] C. Wagg, S. Hann, Y. Kupriyanovich, and S. Li, "Timing of short period water stress determines potato plant growth, yield and tuber quality," *Agricultural Water Management,* vol. 247, pp. 106731, Mar. 2021, doi: 10.1016/j.agwat.2020.106731.

[10] W. Sun, F. Shi, H. Chen, Y. Zhang, Y. Guo, and R. Mao, "Relationship between relative growth rate and C:N:P stoichiometry for the marsh herbaceous plants under water-level stress conditions," *Global Ecology and Conservation,* vol. 25, pp. e01416, Jan. 2021, doi: 10.1016/j.gecco.2020.e01416.

[11] T. Jiang *et al.*, "Simulation of plant height of winter wheat under soil Water stress using modified growth functions," *Agricultural Water Management,* vol. 232, pp. 106066, Apr. 2020, doi: 10.1016/j.agwat.2020.106066.

[12] Y. L. Ju, X. F. Yue, X. F. Zhao, H. Zhao, and Y. L. Fang, "Physiological, micro-morphological and metabolomic analysis of grapevine (Vitis vinifera L.) leaf of plants under water stress," *Plant Physiology and Biochemistry,* vol. 130, pp. 501-510, Sep. 2018, doi: 10.1016/j.plaphy.2018.07.036.

[13] S. O. Ihuoma and C. A. Madramootoo, "Narrow-band reflectance indices for mapping the combined effects of water and nitrogen stress in field grown tomato crops," *Biosystems Engineering,* vol. 192, pp. 133-143, Apr. 2020, doi: 10.1016/j.biosystemseng.2020.01.017.

[14] S. O. Ihuoma and C. A. Madramootoo, "Sensitivity of spectral vegetation indices for monitoring water stress in tomato plants," *Computers and Electronics in Agriculture,* vol. 163, pp. 104860, Aug. 2019, doi: 10.1016/j.compag.2019.104860.

[15] N. Liu *et al.*, "Thermal remote sensing of plant water stress in natural ecosystems," *Forest Ecology and Management,* vol. 476, pp. 118433, Nov. 2020, doi: 10.1016/j.foreco.2020.118433.

[16] A. Khorsandi, A. Hemmat, S. A. Mireei, R. Amirfattahi, and P. Ehsanzadeh, "Plant temperature-based indices using infrared thermography for detecting water status in sesame under greenhouse conditions," *Agricultural Water Management,* vol. 204, pp. 222-233, May 2018, doi: 10.1016/j.agwat.2018.04.012.

[17] B. Das *et al.*, "Evaluation of different water absorption bands, indices and multivariate models for water-deficit stress monitoring in rice using visible-near infrared spectroscopy," *Spectrochimica Acta Part A: Molecular and Biomolecular Spectroscopy,* vol. 247, pp. 119104, Feb. 2021, doi: 10.1016/j.saa.2020.119104.

[18] J. Xia *et al.*, "A cloud computing-based approach using the visible near-infrared spectrum to classify greenhouse tomato plants under water stress," *Computers and Electronics in Agriculture,* vol. 181, pp. 105966, Feb. 2021, doi: 10.1016/j.compag.2020.105966.

[19] A. R. Fonseca, E. J. Fontena, M. Castro, P. Acevedo, J. C. Parra, and M. R. Diaz, "Exploring VIS/NIR reflectance indices for the estimation of water status in highbush blueberry plants grown under full and deficit irrigation," *Scientia Horticulturae,* vol. 256, pp. 108557, Oct. 2019, doi: 10.1016/j.scienta.2019.108557.

[20] B. Li, X. Zhao, Y. Zhang, S. Zhang, and B. Luo, "Prediction and monitoring of leaf water content in soybean plants using terahertz time-domain spectroscopy," *Computers and Electronics in Agriculture,* vol. 170, pp. 105239, Mar. 2020, doi: 10.1016/j.compag.2020.105239.

[21] C. Gameiro, A. B. Utkin, P. Cartaxana, J. M. Silva, and A. R. Matos, "The use of laser induced chlorophyll fluorescence (LIF) as a fast and non-destructive method to investigate water deficit in Arabidopsis," *Agricultural Water Management,* vol. 164, no. 1, pp. 127-136, Jan. 2016, doi: 10.1016/j.agwat.2015.09.008.

[22] A. Elvanidi, N. Katsoulas, K. P. Ferentinos, T. Bartzanas, and C. Kittas, "Hyperspectral machine vision as a tool for water stress severity assessment in soilless tomato crop," *Biosystems Engineering,* vol. 165, pp. 25-35, Jan. 2018, doi: 10.1016/j.biosystemseng.2017.11.002.

[23] Y. Hendrawan and H. Murase, "Bio-inspired feature selection to select informative image features for determining water content of cultured Sunagoke moss," *Expert Systems with Applications,* vol. 38, no. 11, pp. 14321-14335, Oct. 2011, doi: 10.1016/j.eswa.2011.05.097.

[24] Y. Hendrawan, A. Amini, D. M. Maharani, and S. M. Sutan, "Intelligent Non-Invasive Sensing Method in Identifying Coconut (Coco nucifera var. Ebunea) Ripeness Using Computer Vision and Artificial Neural Network," *PERTANIKA Journal of Science & Technology,* vol. 27, no. 3, pp. 1317-1339, Jul. 2019.
[25] Y. Hendrawan, S. Widyaningtyas, and S. Sucipto, "Computer Vision for Purity, Phenol, and pH Detection of Luwak Coffee Green Bean," *TELKOMNIKA Telecommunication, Computing, Electronics and Control,* vol. 17, no. 6, pp. 3073-3085, Dec. 2019, doi: 10.12928/telkomnika.v17i6.12689.
[26] K. Wakamori, R. Mizuno, G. Nakanishi, and H. Mineno, "Multimodal neural network with clustering-based drop for estimating plant water stress," *Computers and Electronics in Agriculture,* vol. 168, pp. 105118, Jan. 2020, doi: 10.1016/j.compag.2019.105118.
[27] Y. Kaneda, S. Shibata, and H. Mineno, "Multi-modal sliding window-based support vector regression for predicting plant water stress," *Knowledge-Based Systems,* vol. 134, pp. 135-148, Oct. 2017, doi: 10.1016/j.knosys.2017.07.028.
[28] D. Moshou, X. E. Pantazi, D. Kateris, and I. Gravalos, "Water stress detection based on optical multisensor fusion with a least squares support vector machine classifier," *Biosystems Engineering,* vol. 117, pp. 15-22, Jan. 2014, doi: 10.1016/j.biosystemseng.2013.07.008.
[29] Y. Hendrawan and H. Murase, "Neural-Intelligent Water Drops algorithm to select relevant textural features for developing precision irrigation system using machine vision," *Computers and Electronics in Agriculture,* vol. 77, pp. 214-228, Jul. 2011, doi: 10.1016/j.compag.2011.05.005.
[30] A. K. Singh, B. Ganapathysubramanian, S. Sarkar, and A. Singh, "Deep Learning for Plant Stress Phenotyping: Trends and Future Perspectives," *Trends in Plant Science,* vol. 23, no. 10, pp. 883-898, Oct. 2018, doi: 10.1016/j.tplants.2018.07.004.
[31] B. S. Anami, N. N. Malvade, and S. Palaiah, "Deep learning approach for recognition and classification of yield affecting paddy crop stresses using field images," *Artificial Intelligence in Agriculture,* vol. 4, pp. 12-20, Apr. 2020, doi: 10.1016/j.aiia.2020.03.001.
[32] S. Azimi, T. Kaur, and T. K. Gandhi, "A deep learning approach to measure stress level in plants due to Nitrogen deficiency," *Measurement,* vol. 173, pp. 108650, Mar. 2021, doi: 10.1016/j.measurement.2020.108650.
[33] X. Hao *et al.*, "MFC-CNN: An automatic grading scheme for light stress levels of lettuce (Lactuca sativa L.) leaves," *Computers and Electronics in Agriculture,* vol. 179, pp. 105847, Dec. 2020, doi: 10.1016/j.compag.2020.105847.
[34] S. K. Noon, M. Amjad, M. A. Qureshi, and A. Mannan, "Use of deep learning techniques for identification of plant leaf stresses: A review," *Sustainable Computing: Informatics and Systems,* vol. 28, pp. 100443, Dec. 2020, doi: 10.1016/j.suscom.2020.100443.
[35] F. Ucar and D. Korkmaz, "COVIDiagnosis-Net: Deep Bayes-SqueezeNet based diagnosis of the coronavirus disease 2019 (COVID-19) from X-ray images," *Medical Hypotheses,* vol. 140, pp. 109761, Jul. 2020, doi: 10.1016/j.mehy.2020.109761.
[36] M. M. Raikar, S. M. Meena, C. Kuchanur, S. Girraddi, and P. Benagi, "Classification and Grading of Okra-ladies finger using Deep Learning," *Procedia Computer Science,* vol. 171, pp. 2380-2389, Aug. 2020, doi: 10.1016/j.procs.2020.04.258.
[37] L. Mkonyi *et al.*, "Early identification of Tuta absoluta in tomato plants using deep learning," *Scientific African,* vol. 10, pp. e00590, Nov. 2020, doi: 10.1016/j.sciaf.2020.e00590.
[38] B. Jiang *et al.*, "Fusion of machine vision technology and AlexNet-CNNs deep learning network for the detection of postharvest apple pesticide residues," *Artificial Intelligence in Agriculture,* vol. 1, pp. 1-8, Mar. 2019, doi: 10.1016/j.aiia.2019.02.001.
[39] K. Thenmozhi and U. S. Redy, "Crop pest classification based on deep convolutional neural network and transfer learning," *Computers and Electronics in Agriculture,* vol. 164, pp. 104906, Sep. 2019, doi: 10.1016/j.compag.2019.104906.
[40] H. Manninen, C. J. Ramlal, A. Singh, S. Rocke, J. Kilter, and M. Landsberg, "Toward automatic condition assessment of high-voltage transmission infrastructure using deep learning techniques," *International Journal of Electrical Power & Energy Systems,* vol. 128, pp. 106726, Jun. 2021, doi: 10.1016/j.ijepes.2020.106726.
[41] A. Miranda, A. Lara, A. Altamirano, C. D. Bella, M. E. Gonzalez, and J. J. Camarero, "Forest browning trends in response to drought in a highly threatened mediterranean landscape of South America," *Ecological Indicators,* vol. 115, pp. 106401, Aug. 2020, doi: 10.1016/j.ecolind.2020.106401.